DOI: 10.1002/ejic.200800559

Nickel Complexes and Cobalt Coordination Polymers with Organochalcogen (S, Se) Ligands Bearing an *N*-Methylimidazole Moiety: Syntheses, Structures, and Properties

Wei-Guo Jia,[a] **Yuan-Biao Huang,**[a] **Yue-Jian Lin,**[a] **Guo-Liang Wang,**[a] **and Guo-Xin Jin***[a]

Dedicated to Professor Xi-Yan Lu on the occasion of his 80th birthday

Keywords: Chalcogens / Nickel / Cobalt / Polymerization

The organochalcogen ligands (S, Se) derived from 3-methylimidazole-2-thione/selone groups mbit (**2a**), mbis (**2b**), ebit (**2c**), and ebis (**2d**) [mbit = 1,1′-methylenebis(1,3-dihydro-3-methyl-2*H*-imidazole-2-thione), mbis = 1,1′-methylenebis(1,3-dihydro-3-methyl-2*H*-imidazole-2-selone), ebit = 1,1′-(1,2-ethanediyl)bis(1,3-dihydro-3-methyl-1*H*-imidazole-2-thione), ebis = 1,1′-(1,2-ethanediyl)bis(1,3-dihydro-3-methyl-1*H*-imidazole-2-selone)] were synthesized and characterized. Mononuclear Ni^{II} complexes $NiBr_2$mbit (**3a**), $NiBr_2$mbis (**3b**), $NiBr_2$ebit (**3c**), and $NiBr_2$ebis (**3d**) were obtained by the reactions of $Ni(PPh_3)_2Br_2$ with **2a**, **2b**, **2c**, and **2d**, respectively. However, when the corresponding ligands **2a**, **2b**, **2c**, and **2d** were treated with $CoCl_2$ in thf solution Co^{II} 1D coordination polymers $(CoCl_2mbit)_n$ (**4a**), $(CoCl_2mbis)_n$ (**4b**), $(CoCl_2ebit)_n$ (**4c**), and $(CoCl_2ebis)_n$ (**4d**) were obtained. All compounds were fully characterized by IR spectroscopy and elemental analysis. The crystal structures of **2c**, **3a**, **3b**, **3c**, **4a**, **4b**, and **4c** were determined by X-ray crystallography. The local geometry around the nickel atom in complexes **3a–c** was distorted tetrahedron with coordinated S(Se) and two Br atoms, and the organochalcogen ligands form an eight- or a nine-membered ring with the nickel atom included. The cobalt atom coordination polymers **4a** and **4b** coexist as left-handed and right-handed helical chains, but **4c** formed a zigzag chain with a CH_3CN solvent molecule taken up in the channel structure. After activation with methylaluminoxane (MAO), the nickel complexes exhibited high activities for addition polymerization of norbornene (1.42×10^8 g PNB-mol^{-1} Nih^{-1} for **3a**). The effects of the Al/Ni ratio, reaction temperature, and reaction time to norbornene polymerization were also investigated.

Introduction

There has been a growing interest in the chemistry of multitopic ligands with “soft” Lewis donors for fundamental studies in the coordination and supramolecular chemistry.[1] In particular, the systematic design and exploration of sulfur-containing ligands[2] with metals have been examined for studies in bioinorganic chemistry and for their ability to form diverse coordination network architectures.[3] A family of compounds bearing bis(thioimidazolyl)methane are attractive owing to both their potential biomedical applications and their potential utility in fundamental coordination chemistry.[4] There are different coordination models for different metals with bis(thioimidazolyl)methane ligands (Scheme 1). Williams reported that the $SbCl_3$mbit complex adopts a bidentate model in which the ligand forms an eight-membered ring with the metal included [Scheme 1, (a)].[4d] In the structure of the $SbCl_3$mbit complex, the antimony coordination center was in a distorted square pyramid, and the base was made up of three chlorine atoms and one sulfur atom; however, upon inspection of intermolecular contacts, instead of a lone pair of electrons occupying the space below the basal plane of the square pyramid, there is a sulfur atom from a neighboring molecule bridging the antimony center at a distance of 3.41 Å (well within the sum of the van der Waal’s radii of 4.0 Å). Thus, the structure of the $SbCl_3$mbit complex is better described as a polymeric zigzag chain of distorted octahedra linked through long sulfur bridges *cis* to each other. The $PbCl_2$mbit complex, which is the first instance where mbit is shown to act a bridging ligand, was also synthesized by Williams in boiling water.[4c] A single-crystal X-ray study of the $PbCl_2$mbit complex revealed a unique cross-linked polymeric structure composed of very distorted $PbCl_4S_2$ octahedra sharing common edges through long Pb–Cl brid-

---

[a] Shanghai Key Laboratory of Molecular Catalysis and Innovative Material, Department of Chemistry, Fudan University,
Shanghai 200433, P. R. China
Fax: +86-21-65643776
E-mail: gxjin@fudan.edu.cn

ges. The bridging pairs of Cl atoms are displaced *cis* to each other in the coordination sphere of lead, thus creating twisted polymeric Pb–Cl strands running along the *c* axis. In the direction of the *b* axis, the strands are further linked by mbit ligands acting as bridges between neighboring twisted strands created by the lead chloride bonds. Deplano reported the tin $Sn(mbit)_2I_4$ complex prepared by reaction of the adduct of mbit·$2I_2$ and tin powder under mild conditions.[4a] The X-ray study showed that the compound consists of a $[Sn(mbit)_2I_2]^{2+}$ cation that interacts with two disordered diiodine molecules. In the cation, the Sn atom lying on a symmetry center exhibits a slightly distorted octahedral coordination with two iodides at the apices in a *trans* position and with two mbit molecules acting as bidentate chelating ligands through the S atom and forming an eight-membered ring with the tin metal atom included [Scheme 1, (c)]. Gardinier found that coordination polymers of the type $\{[Ag(mbit)_2]X\}_n$ (X = BF_4, PF_6) are formed by a bridging mbit ligand between tetrahedral silver centers giving 2D cationic sheets composed of AgS_4 linkages; the anions are sandwiched between sheets [Scheme 1, (d)].[1b] Hill obtained the first rhodium complexes of the $H_2C(Mt)_2$ (Mt = methimazolyl) and $H_2B(Mt)_2$ ligands.[4g] In these rhodium complexes, the geometry imposed by the $H_2A(Mt)_2Rh$ (A = B, C^+) metallacycle positions one A–H bond proximal to the rhodium center [Scheme 1, (e)]. Santos reported a rhenium(I) tricarbonyl complex bearing bis(2-mercaptoimidazolyl)methane ligands.[4h] The rhenium atom in the rhenium(I) tricarbonyl complex adopts a slightly distorted octahedral coordination with a facial arrangement of the carbonyl ligands. The three remaining coordination positions are occupied by the two thione sulfur atoms from the anchor ligands and a bromide ligand [Scheme 1, (f)].

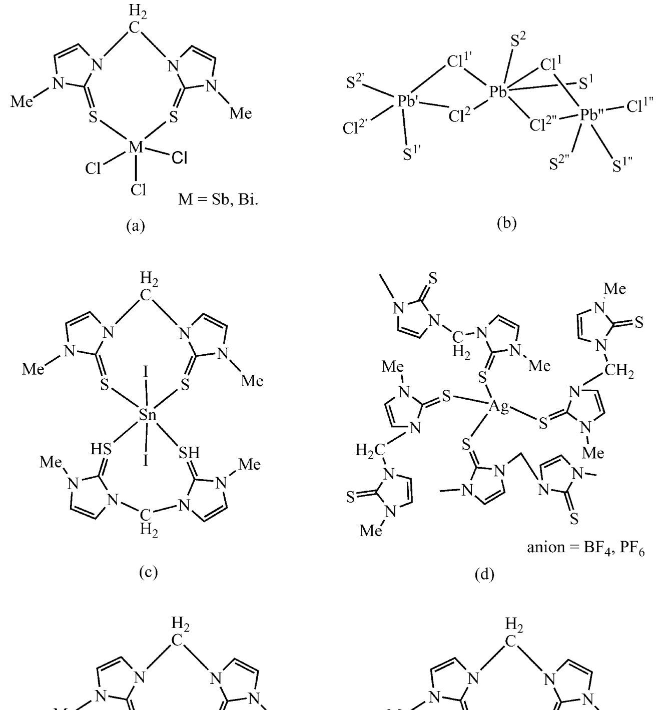

Scheme 1. The coordination models of the mbit ligand.

Dithiolene nickel and cobalt complexes are currently being extensively investigated from the viewpoint of catalytic, optical, magnetic, and conductivity studies.[5] Whereas the $[S_2]$ bidentate ligands are ubiquitous,[4] analogous ligands that feature an $[Se_2]$ donor array are uncommon. The selenium analogues are expected to be more nucleophilic than their sulfur counterparts, which should result in a stronger coordination bond.[6] The changes in flexibility, length, and symmetry of the organic ligands can result in a remarkable class of materials bearing diverse architectures and functions. Thus, the construction of target molecules with properties mentioned above is a challenge for synthetic chemists. To achieve the desired complexes and networks, the important family of multidentate S(Se)-donor ligands are often applied as bridging ligands to construct novel coordination polymers due to their versatile coordination modes. Therefore, the design of such organochalcogen (S, Se) compounds bearing *N*-methylimidazole ligands are very attractive from the organometallic and application points of view, and the complexes containing these functional group strongly bound to late transition metals are of considerable interest.

The PNB (polynorbornene) formed by addition polymerization displays a characteristic rigid random coil conformation, which shows restricted rotation about the main chain and exhibits strong thermal stability ($T_g > 350$ °C). In addition, it has excellent dielectric properties, optical transparency, and unusual transport properties. This has prompted many chemists to study the norbornene addition polymerization reaction. Up to now, catalytic systems based on titanium,[7] zirconium,[8] hafnium,[9] vanadium,[10] cobalt,[11] chromium,[11a,12] nickel,[12b,13] palladium,[14] and copper[13p,15a–15d] complexes have been mainly reported for the addition polymerization of norbornene. Recently, rare-earth metals were also used in such a reaction, although with a low activity.[15e] After Deming and Novak introduced the first nickel complex for the addition polymerization of norbornene,[16] nickel complexes bearing N,O and N,N ligands were then explored;[12b,13] however, nickel complexes bearing organochalcogen S(Se) ligands for the polymerization have been reported rarely.[13,17]

In this paper, we report the convenient synthesis of mononuclear Ni dichalcogenolato complexes and cobalt coordination polymers by using the reaction of organochalcogen (S, Se) ligands bearing *N*-methylimidazole with $Ni(PPh_3)_2Br_2$ and $CoCl_2$, respectively. In the presence of methylaluminoxane (MAO), the four mononuclear nickel complexes **3a–d** have proved to be efficient for the addition polymerization of norbornene. Ultrahigh catalytic activity

(1.42×10^8 gPNBmol^{-1} Nih^{-1} for **3a**) was observed for the addition polymerization of norbornene by using the nickel(II)/MAO system.

Results and Discussion

Synthesis and Characterization of Ligands and Ni^{II} Complexes and Co^{II} 1D Coordination Polymers

As outlined in Scheme 2, the bidentate organochalcogen (S, Se) ligands bearing *N*-methylimidazole **2a–d** were easily prepared with moderate yields by the reaction of methylene- and ethylene-bridged methylimidazolium dibromide with sulfur or selenium powder in MeOH solution, through a slightly modified literature procedure for the synthesis of ligand **2a**.[4d] All the ligands were air and moisture stable, and they were soluble in common organic solvents such as CH_2Cl_2, $CHCl_3$, and thf. Ligands **2a–d** were characterized by NMR and IR spectroscopy as well as by elemental analysis. The formation of **2b** was confirmed by the appearance of the ^{1}H signals at 3.67, 6.54, 6.78, and 8.02 ppm, which can be assigned to the methyl, CH_2, and two olefinic H protons of the mbis ligand, respectively, and the IR spectra exhibit intense N–C–N and C=S stretching at about 1566, 1194, and 1128 cm^{-1} on the basis of the reported values for analogous modes in mbit. Similarly, the resonances at 3.61, 4.49, 6.60 and at 3.69, 4.62, 6.80 ppm in the ^{1}H NMR spectrum of **2c** and **2d**, respectively, confirm their structures. The IR spectra exhibit intense N–C–N and C=S stretching at about 1562, 1192, and 1136 cm^{-1} for **2c** and at 1560, 1171, and 1126 cm^{-1} for **2d**. The ^{13}C NMR spectra show a singlet at about 158 ppm for **2a** and **2c** and at 162 ppm for **2b** and **2d**, which also prove the existence of C=E (E = S, Se) groups.

A single crystal of **2c** suitable for X-ray diffraction was determined (Figure 1), which suggests the whole molecule possesses a center of symmetry. The two imidazole-2-thione ring moieties are *trans* to each other, and the bridging chain moiety -CH_2CH_2- adopts an antiperiplanar conformation; the C=S bond length is 1.677(3) Å, which possess a typical double bond.

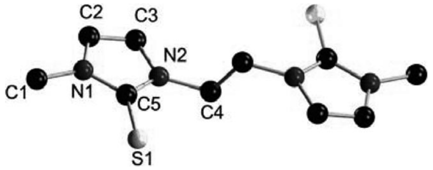

Figure 1. Molecular structure of **2c**; all the hydrogen atoms are omitted for clarity. Selected distances [Å] and angles [°]: C5–S1 1.677(3), C2–C3 1.323(5); N1–C5–N2 105.4(3), N1–C5–S1 127.4(3), N2–C5–S1 127.2(2).

Dichloromethane solutions of equimolar amounts of $Ni(PPh_3)Br_2$ and each of the ligands **2a–d** were stirred at room temperature under an atmosphere of nitrogen for 10 h to produce compounds **3a–d** in yields of 75, 40, 60, and 32%, respectively (Scheme 2). The compounds with sulfur ligands are stable to air and moisture, whereas those with selenium ligands are very sensitive to air and moisture. All the nickel complexes are moderately soluble in polar solvent such as MeCN, DMSO, and DMF, but insoluble in common organic solvents such as CH_2Cl_2, $CHCl_3$, thf, and toluene. The NMR spectra of four nickel complexes are not informative because of the interfering effect caused by their paramagnetism. This phenomenon can be seen from other tetrahedral nickel complexes.[18] In comparison to the IR spectra of the corresponding free ligands, all the Ni^{II} complexes have slight changes. The IR bands that should be of most interest in investigating the coordination mode of the ligand are *ν*(NCN) and *ν*(C=S) or *ν*(C=Se).[19] The IR spectrum of **3a** in the solid state exhibited intense N–C–N and C=S stretching at about 1570, 1195, and 1153 cm^{-1}. The IR spectra of complex **3b** in the solid state exhibited intense N–C–N and C=Se stretching at about 1570, 1194, and 1133 cm^{-1}, which is in agreement with the data of the structures.[19] Bands at around 1565, 1193, and 1146 cm^{-1} in the

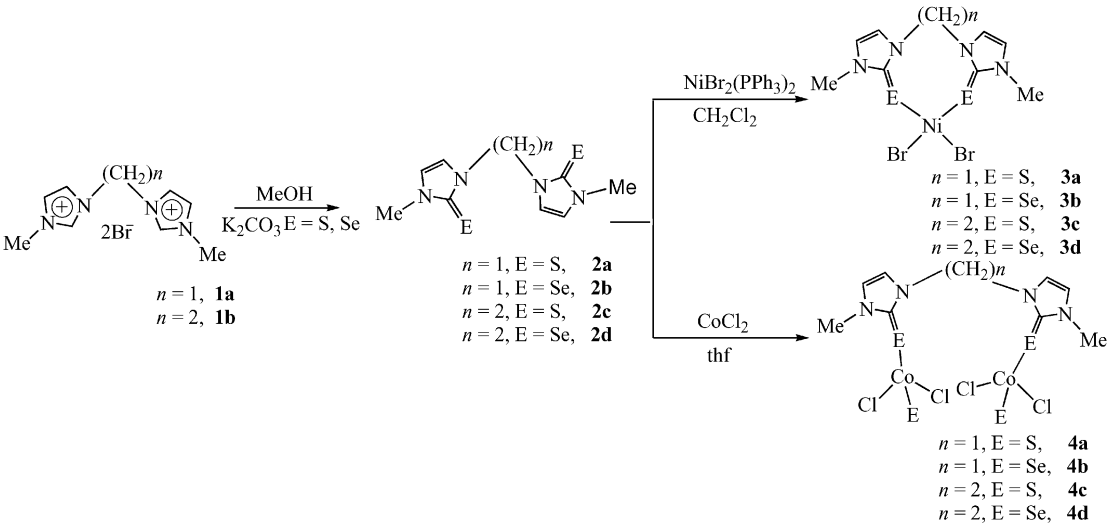

Scheme 2. Synthesis of ligands **2**, Ni^{II} complexes **3**, and Co^{II} coordination polymers **4**.

IR spectra can be assigned to the N–C–N and C=S stretching for **3c**. The IR spectra of **3d** show the N–C–N and C=S stretching at around 1566, 1177, and 1126 cm^{-1}. Except for complexes **3a**, the *v*(NCN) shift a higher frequencies and simultaneously the one *v* [C=S(Se)] shift a higher frequencies and the other to lower frequencies.

The fine bright-green crystals of **3a**–**c** were obtained by vapor diffusion of an Et_2O solution into a MeCN solution. The crystallographic data for compounds **2c** and **3a**–**c** are summarized in Table 3. The molecular crystal structure of **3a** was determined by X-ray crystallographic diffraction [Figure 2a]. The structure of **3a** is solved in the orthorhombic crystal system and *Pnma* space group. As can be seen, the coordination geometry of the central nickel center can be best described as a distorted tetrahedron with two Br atoms and two S atoms [S1–Ni1–S1 108.33(7)°, S1–Ni1–Br1 103.87(3)°, S1–Ni1–Br2 105.12(3)°, Br1–Ni1–Br2 129.37(4)°]. The ligand with the nickel center forms an eight-membered macrocyclic ring, which shows a chair conformation. The Ni–S bond length is 2.2839(12) Å, which is significantly longer than that of the corresponding Ni^{II} dithiolene complexes with five-membered rings [$CpNi\{S_2C_2S_2(CH_2)_3\}$][20] [2.128(4) and 2.129(4) Å], CpNi(dddt)[21] [2.125(2) and 2.127(2) Å], and CpNi(bdt)[21] [2.1205(13) and 2.1280(13) Å], but similar to the complexes with eight-membered rings $Tm^{R}NiCl$[22] [Tm = tris(mercaptoimidazolyl)borate, 2.3000(7) Å for R = Ph and 2.2866(8) Å for R = 2,6-$iPr_2C_6H_3$], which have the mercaptoimidazole groups in the complex. The C1–S1 distance is 1.701(4) Å, which is longer than a typical C=S bond but shorter than the C–S bond. Another remarkable feature of **3a** is that the curvilinear shapes form an interesting stacking structure along the *c* axis. As shown in Figure 2b, the shapes are identified within every layer, which are most probably stabilized by two almost linear C–H···Br weak hydrogen bonds with an H···Br distance of 2.750(1) Å, which play a crucial role in halogenated molecules in the solid state.[20]

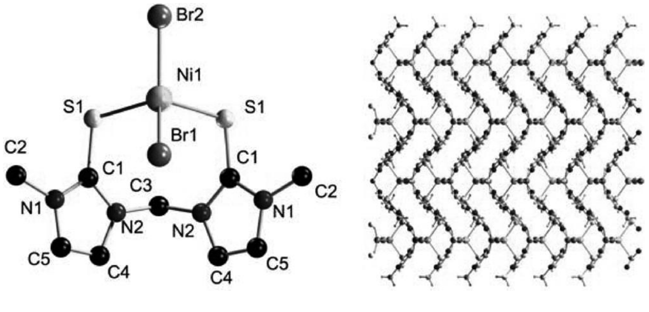

(a) (b)

Figure 2. (a) Molecular structure of **3a**; all hydrogen atoms are omitted for clarity. Selected distances [Å] and angles [°]: Ni1–S1 2.2839(12), Ni1–Br1 2.3860(11), Ni1–Br2 2.3284(12) C1–S1 1.701(4); S1–Ni1–S1 108.33(7), S1–Ni1–Br1 103.87(3), S1–Ni1–Br2 105.12(3), Br1–Ni1–Br2 129.37(4). (b) Crystal structure of **3a** viewed down the *c* axis.

The solid structure of **3b** (Figure 3) is very similar to that of complex **3a**, which also possesses a chair conformation an eight-membered macrocyclic ring configuration. As expected, the coordination geometry around the Ni centers can be seen as a distorted tetrahedron with two Br atoms and two Se atoms [Se1–Ni1–Se1 106.05(4)°, Se1–Ni1–Br1 105.12(2)°, Se1–Ni1–Br2 103.142° and Br1–Ni1–Br2 132.10(4)°]. The distance between Se and Ni is 2.3941(8) Å, which is significantly longer than the Ni–S bond length [2.2839(12) Å] of complex **3a** and that in the corresponding Ni^{II} dithiolene complexes with five-membered rings CpNi(ddds)[21] [2.233(3) and 2.249(2) Å], CpNi(bds)[21] [2.2500(18) and 2.2393(19) Å], and CpNi(dsit)[23] [2.250(13) and 2.250(18) Å], but shorter than the complex [Tse^{Mes}]-NiNO [2.4489(3) Å],[24] which has three eight-membered rings in the structure.

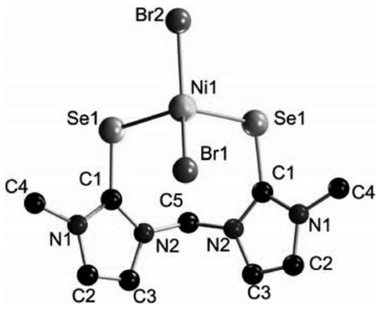

Figure 3. Molecular structure of **3b**; all hydrogen atoms are omitted for clarity. Selected distances [Å] and angles [°]: Ni1–Se1 2.3941(8), Ni1–Br1 2.3944(10), Ni1–Br2 2.3402(10), C1–Se1 1.871(3); Se1–Ni1–Se1 106.05(4), Se1–Ni1–Br1 105.12(2), Se1–Ni1–Br2 103.14(2), Br1–Ni1–Br2 132.10(4).

The molecular structure of complex **3c**, together with selected bond lengths and angles, are depicted in Figure 4. Although the ligand with the metal forms a nine-membered macrocyclic ring, the molecular structure of complex **3c** is also similar to that of complexes **3a** and **3b**. Both of the Ni1–S1 [2.3155(18) Å] and Ni1–S2 [2.2861(18) Å] bond lengths are longer than that in complex **3a** [2.2839(12) Å], and both of the C–S distances [C1–S1 1.716(6) Å, C7–S2 1.697(6) Å] are longer than the C=S bond of the corresponding ligand **2c** [1.677(3) Å] as a result of the back donation from the metal to the mercaptoimidazole group.

Interestingly, the reaction of the corresponding **2a**–**d** ligands with $CoCl_2$ (1:1 ratio) in thf resulted in blue Co^{II} 1D coordination polymers **4a**–**d**, which were different from nickel complexes **3a**–**d** (Scheme 2). All the Co^{II} 1D coordination polymers are moderately soluble in MeCN solution. Similar to Ni^{II} complexes **3a**–**d**, ^1H NMR spectroscopic analysis of the four Co^{II} 1D coordination polymers in CD_3CN failed due to the paramagnetic character of the Co^{II} coordination model. The assignments of the IR bands may be difficult, as extensive coupling may occur.[4] The IR spectra of the Co^{II} coordination polymers **4a**–**c** have lower frequencies of *v*(NCN) and *v*[C=S(Se)]; however, in **4d** these bands are shifted to higher frequencies relative to those of the free ligands (see Experimental Section).

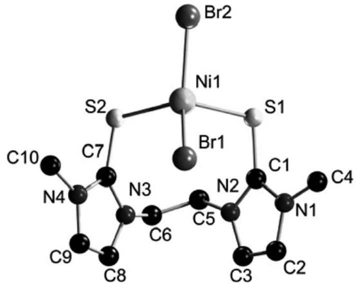

Figure 4. Molecular structure of **3c**; all hydrogen atoms are omitted for clarity. Selected distances [Å] and angles [°]: Ni1–S1 2.3155(18), Ni1–S2 2.2861(18), Ni1–Br1 2.3963(11), Ni1–Br2 2.3781(12) C1–S1 1.716(6), C7–S2 1.697(6); S1–Ni1–S2 113.76(9), S1–Ni1–Br1 101.84(6), S1–Ni1–Br2 95.11(5), S2–Ni1–Br1 105.96(5), S2–Ni1–Br2 101.44(5), Br1–Ni1–Br2 138.20(4), C6–C5–N2 118.5(7), C5–C6–N3 119.1(6).

Blue crystals of **4a**–**c** suitable for X-ray crystallographic diffraction were obtained by vapor diffusion of an Et_2O solution into a MeCN solution. The crystallographic data for compounds **4a**–**c** are summarized in Table 4. As can be seen from Figure 5, crystal **4a** was found to comprise a 1D polymer of [$(CoCl_2mbit)_n$] units. Each cobalt ion is coordinated to two chlorine atoms and two S atoms of different mbit ligands to result in a highly distorted tetrahedral geometry. The two imidazole rings bridged by C4 are oriented essentially orthogonal to each other (91.1°), and the dihedral angel of the two imidazole rings bridged by the $CoCl_2$ unit is 106.4°. The adjacent Co atoms are located in a *trans* geometry by the S bridged ligands, which is different with the nickel complexes (the S in the same ligand are in a *cis* conformation). The distance of the adjacent Co···Co connected by the S bridge are rather far apart [7.6337(26) Å]. The Co–S bond length is 2.3488(19) Å, which is longer than the Ni–S bond of the corresponding Ni complex **3a** [2.2839(12) Å]. Similar to nickel complexes **3a** and **3c**, the C1–S1 bond length [1.721(6) Å] is between that of a single and double bond. This bridging S donor mediates the formation of infinite helical chains that extend along the crystallographic *c* axis [Figure 6a], Furthermore, weak hydrogen-bonding interactions exist between the chlorine atoms and the hydrogen atoms of the C4 and imidazole rings with C–H···Cl distances in the range of 2.6845 to 2.8225 Å, which further stabilizes the supermolecular network structure.

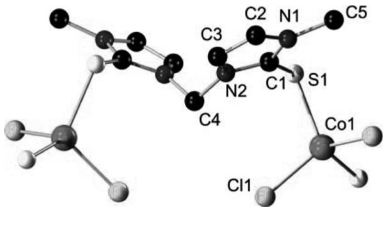

Figure 5. The structure of the repeating unit of **4a**; all hydrogen atoms are omitted for clarity. Selected distances [Å] and angles [°]: Co1–S1 2.3488(19), Co1–Cl1 2.249(2), C1–S1 1.721(6), Cl1–Co1–Cl1A 113.83(12), Cl1–Co1–S1 111.80(7), Cl1–Co1–S1A 105.50(7), S1–Co1–S1A 108.38(9).

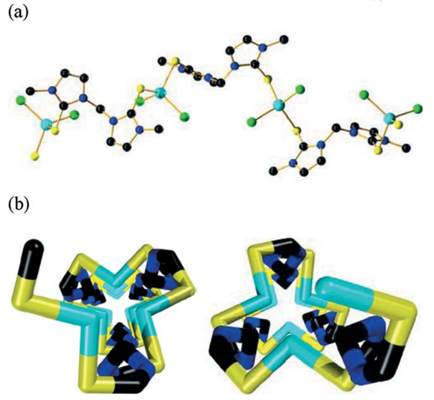

Figure 6. (a) X-ray crystal structure of the chain of the $(CoCl_2mbit)_n$ (**4a**) coordination polymer (light blue = Co, green = Cl, yellow = S, black = C, dark blue = N); (b) View of the left and right helical chains in Co coordination polymer **4a** along the *c* axis (Cl atoms have been omitted for clarity; light blue = Co, yellow = S, black = C, dark blue = N).

The solid structure of blue Co coordination polymer **4b** [$(CoCl_2mbis)_n$] connected by the Se atoms is very similar to that of crystal **4a** (Figure 7). The repeating unit is $CoCl_2$ and mbis ligands. As expected, the coordination geometry around the Co centers connected by two chlorine atoms and two Se atoms of different mbis ligands can be seen as distorted tetrahedral geometry. The distance of the Co···Co bond connected by the Se bridge is 7.6602(129) Å, which is longer than that of **4a**. The Co–Se bond length is 2.447(4) Å, which is longer than that of the Ni–S bond of the corresponding Ni complex **3b** [2.3941(8) Å]. Similar to nickel complex **3b**, the C1–Se1 bond length [1.854(10) Å] is between that of a single and double bond. The dihedral angel of the two imidazole rings bridged by C4 and the $CoCl_2$ unit is 124.7 and 93.8°, respectively. This bridging S donor mediates the formation of infinite helical chains that extend along the crystallographic *c* axis [Figure 8a]. Furthermore, the supermolecular network structure was further stabilized by weak hydrogen-bonding interactions between the chlorine atoms and the hydrogen atoms of C4 and the imidazole rings with C–H···Cl distances in the range of 2.6793 to 2.8885 Å.

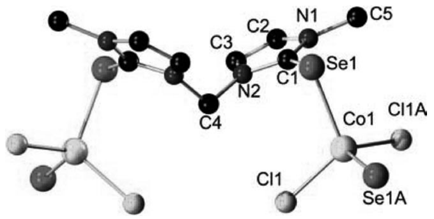

Figure 7. The structure of the repeating unit of **4b**; all hydrogen atoms are omitted for clarity. Selected distances [Å] and angles [°]: Co1–Se1 2.447(4), Co1–Cl1 2.247(4), C1–Se1 1.854(10), Cl1–Co1–Cl1A 113.3(2), Cl1–Co1–Se1 112.98(14), Cl1–Co1–Se1A 106.55(10), Se1–Co1–Se1A 104.18(9).

Both mbit and mbis ligands behave in an *exo* bidentate mode and lie on the two sides of the polymer chain in complexes **4a** and **4b**.[25] The most fascinating structural feature

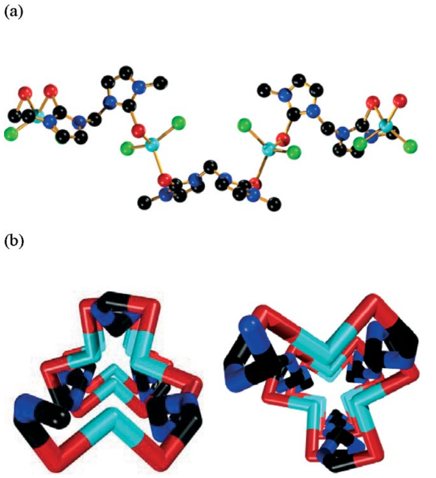

Figure 8. (a) X-ray crystal structure of the chain of the $(CoCl_2mbis)_n$ (**4b**) coordination polymer (light blue = Co, green = Cl, red = Se, black = C, dark blue = N); (b) view of the left and right helical chains in Co coordination polymer **4b** along the *c* axis (Cl atoms have been omitted for clarity; light blue = Co, red = Se, black = C, dark blue = N).

is that there are two different chirality structures in complexes **4a** [Figure 6b] and **4b** [Figure 8b]: one is left handed, whereas the other is right handed, though they have the same components and linking sequence.

The solid structure of blue Co crystal **4c** (Figure 9) is also similar to that of **4a** and **4b**. However, the structure was solved in the space group $P2_1/n$, which is different from **4a** (*R*-3*c*) and **4b** (*R*-3*c*). It contains polymeric $(CoCl_2ebit)_n$ molecules forming zigzag chains extending in the crystal lattice along the crystallographic *b* direction of a monoclinic lattice (Figure 10). There is no existing helical chain that is different from that in **4a** and **4b** due to the ethylidene bridged ligand of **4c**, which results in the two S atoms in the same ligand being located on the same side. As viewed down the crystal packing structure (Figure 11), the CH_3CN solvent molecule, which is connected to the CH_3 group of the imidazole ring by a hydrogen bond [C–H···N (2.523 Å)], occupies the channel formed by the 3D structure. Furthermore, the supermolecular network structure was further stabilized by the hydrogen-bonding interactions between the chlorine atoms and the hydrogen atoms of the imidazole rings with C–H···Cl distances in the range 2.7293–3.0344 Å and the C–H···S (2.813 Å) interaction of the S atoms with the CH_3 groups of the imidazole rings (Figure 11). The cobalt ion is also coordinated to two chlorine atoms and two S atoms of different ebit ligands in a highly distorted tetrahedral geometry. The dihedral angel of the two imidazole rings bridge by ethylidene ligands and the $CoCl_2$ unit is 47 and 63.9°, respectively, which is lower than that of crystals **4a** and **4b**. Although the two neighboring cobalt atoms are almost on the same side, due to the longer connected ethylidene ligands, the distance of the Co···Co bond connected by the S bridge is longer [8.4121(50) Å] than that of **4a** and **4b**. The Co–S bond length is 2.3362(19) Å, which is longer than that of the Ni–S bond of the corresponding Ni complex **3c** [2.3155(18) Å]. Similar to nickel complexes **3a** and **3c**, the C1–S1 bond length [1.709(5) Å] is between that of a single and double bond [**2c** 1.677(3) Å].

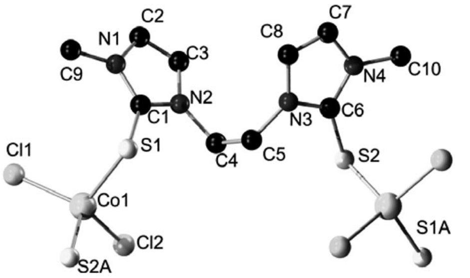

Figure 9. The structure of the repeating unit of **4c**; all hydrogen atoms are omitted for clarity. Selected distances [Å] and angles [°]: Co1–S1 2.3362(19), Co1–S2A 2.328(2), Co1–Cl1 2.2421(18), Co1–Cl2 2.2527(19), C1–S1 1.709(5), C6–S1 1.706(5), Cl1–Co1–Cl2 109.92(7), Cl1–Co1–S2A 112.63(8), Cl2–Co1–S2A 111.54(7), Cl1–Co1–S1 112.40(6), Cl2–Co1–S1 115.21(8), S2A–Co1–S1 94.44(5).

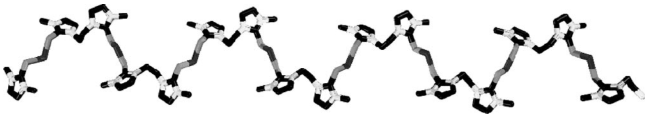

Figure 10. X-ray crystal structure of the zigzag chain of the $(CoCl_2ebit)_n$ (**4c**) coordination polymer along the *b* axis (Cl atoms and CH_3CN molecules have been omitted for clarity; dark gray = Co, light gray = S, black = C, white = N).

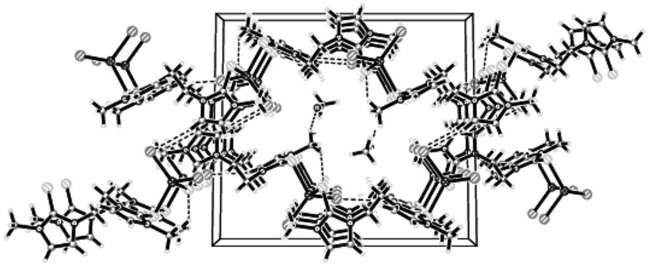

Figure 11. View of the crystal packing of **4c** with CH_3CN trapped within the channel and hydrogen-bonding contacts along the *a* axis.

Nickel Complexes for Polymerization of Norbornene

To the best of our knowledge, the most active system for norbornene polymerization are nickel complexes bearing N,O and N,N ligands;[12b,13] however, the use of nickel complexes bearing soft coordination atom S(Se) ligands in norbornene (NB) polymerizations is rare.[13,17]

Preliminary experiments have indicated that neither Ni complexes **3a–d** nor MAO alone is able to catalyze norbornene polymerization. Interestingly, in combination with MAO, Ni complexes **3a–d** exhibit extremely high catalytic activity for NB polymerization under moderate conditions. Results for the NB polymerization by using different nickel complexes are summarized in Table 1. After activation of

MAO, nickel complexes **3a**–**d** showed high activities (0.026–1.42×10^{8} gPNBmol^{-1} Nih^{-1}; Table 1, Entries 1–4), and in particular, complex **3a** exhibits the highest activity (1.42×10^{8} gPNBmol^{-1} Nih^{-1}) under the same conditions. This is similar to the nickel complex bearing 2′-(4′,6′-di-*tert*-butylhydroxyphenyl)-1,4,5-triphenylimidazole,[13p] but higher than the other nickel complexes bearing N,O and N,N ligands.[12b,13a–13p] The catalytic results indicate that the structure of the complexes have an effect on the catalytic activity. The activity of complex **3a** (coordinated S atom, eight-membered ring; 1.42×10^{8} gPNBmol^{-1} Nih^{-1}) is higher than complex **3b** (coordinated Se atom, eight-membered ring; 0.44×10^{8} gPNBmol^{-1} Nih^{-1}) and complex **3c** (coordinated S atom, nine-membered ring; 0.87×10^{8} gPNBmol^{-1} Nih^{-1}) under the same conditions. The Se atom has a higher electron-donating ability to the metal center than the S atom, and the eight- and nine-membered rings may affect the catalytic activity of norbornene polymerization.[17b,17c]

Table 1. Norbornene polymerization for the **3a**–**d**/MAO catalytic system.[a]

Run	Al/Ni	T [°C]	Yield [g]	Conv.[%]	Activity[b]	M_v[c]
1 (**3a**)	3000	25	2.369	63.01	1.42	1.05
2 (**3b**)	3000	25	0.338	8.99	0.44	1.00
3 (**3c**)	3000	25	1.449	38.54	0.87	0.85
4 (**3d**)	3000	25	0.044	1.17	0.026	0.92

[a] Polymerization conditions: [Ni] = 0.2 μmol, [NB] = 3.76 g; t = 5 min; V_{total} = 20 mL; solvent: chlorobenzene. [b] 10^{8} gGPNBmol^{-1} Nih^{-1}. [c] 10^{6} g mol^{-1}.

To investigate the reaction parameters affecting vinyl polymerization of norbornene, catalyst precursor **3a** with the highest activity of the four nickel complexes (**3a**–**d**) was the best choice to evaluate the effects of the ratios of MAO and nickel complexes (expressed as Al/Ni) and the reaction temperature on the activity and polymer molecular weights. As shown in Table 2, when Al/Ni = 500, there is almost no polymer. The catalytic activity increases from 0.304×10^{7} to 1.42×10^{8} gPNBmol^{-1} Nih^{-1} when Al/Ni increases from 1000:1 to 3000:1. In contrast, the viscosity-averaged molecular weight (M_v) of the polymer decreases from 1.10×10^{6} to 1.05×10^{6} g mol^{-1} with an increase in the molar ratio of MAO/**3a** due to the chain transfer to MAO.[17] However, when Al/Ni is increased further, the activity decreases to 1.36×10^{8} gPNBmol^{-1} Nih^{-1} (Al/Ni = 4000), whereas the viscosity-averaged molecular weight of the polymer also decreases.

The high viscosity of the reaction medium in the polymerization system did not allow efficient stirring within 3 min, and the conversion was up to 63.01% after 5 min (**3a**; Table 1, Entry 1). The influence of reaction time on polymerization is summarized in Table 2, Entries 11–14. The conversion increased by increasing the reaction time, and the conversion was almost 100% after 24 h. These results clearly indicate that the catalyst was still active after 24 h.

The polymerization temperature also affects considerably the catalytic activities and molecular weight of complex **3a** (Table 2). With an increase in the reaction temperature, the catalytic activities first increase and then decrease. The maximum value for the activities was obtained at 25 °C. When the reaction temperature was increased further, the catalytic activity decreased. There is almost no polymer formation at 80 °C, which may be attributed to decomposition of the nickel complex at higher temperatures.

Table 2. Norbornene polymerization for the **3a**/MAO catalytic system.[a]

Run	Al/Ni	T [°C]	Yield [g]	Conv. [%]	Activity[b]	M_v[c]
5	500	25	Trace			
6	1000	25	0.051	1.36	0.0304	1.10
7	1500	25	0.370	9.84	0.221	0.62
8	2000	25	2.223	59.31	1.32	0.95
9	2500	25	2.243	59.65	1.35	0.71[d]
10	4000	25	2.264	60.21	1.36	0.86
11[e]	3000	25	3.190	84.85	0.16	1.17
12[f]	3000	25	3.247	86.35	0.03	1.20
13[g]	3000	25	3.419	90.94	0.01	1.33
14[h]	3000	25	3.743	99.56	0.008	1.42
15	3000	4	0.417	11.10	0.25	0.30
16	3000	40	0.383	10.19	0.229	1.02
17	3000	57	0.381	10.13	0.222	2.29
18	3000	80	Trace			

[a] Polymerization conditions: [Ni] = 0.2 μmol, [NB] = 3.76 g; t = 5 min; V_{total} = 20 mL; solvent: chlorobenzene. [b] 10^{8} gPNBmol^{-1} Nih^{-1}. [c] 10^{6} g mol^{-1}. [d] Not completely dissolved. [e] t = 1 h. [f] t = 6 h. [g] t = 12 h. [h] t = 24 h.

The microstructure of the obtained polynorbornene was characterized by NMR and IR spectroscopy. The ^{1}H NMR spectra show signals in the 0.9–3.0 ppm range (m, maxima at 1.13 1.56 2.11 2.31) and the ^{13}C NMR spectra show signal maxima at 29–33, 34–37, 38–42, 46–53 ppm, which indicated the absence of a double bond in the polymer and that the polymerization goes through a vinyl-type mechanism. The IR absorption peak at about 943 cm^{-1} can be assigned to the ring system of bicyclo[2.2.1]hept-2-ene, as noted by Kenndy.[26] There were no absorptions at 1680–1620 cm^{-1}, especially at 960 cm^{-1} and 735 cm^{-1}, which are characteristic of the ring-opening metathesis polymerization (ROMP) structure of polynorbornenes.[13e,27] Those spectra are typical of a vinyl-type structure. All polynorbornenes are soluble at room temperature in chlorobenzene and cyclohexane, which indicate atactic stereoregularity.[28]

Conclusions

A series of mononuclear Ni^{II} complexes **3a**–**d** with eight- or nine-membered rings were obtained by the reaction of NiBr$_2$(PPh$_3$)$_2$ and organochalcogen (S, Se) ligands bearing *N*-methylimidazole, mbit (**2a**), mbis (**2b**), ebit (**2c**), and ebis (**2d**). However, the methylene-bridged organochalcogen (S, Se) ligands bearing *N*-methylimidazole, **2a** and **2b**, react with CoCl$_2$ in thf to produce chiral helical-chain (left-handed and right-handed helical chains) coordination polymers **4a** and **4b**, whereas the ethylidene bridged ligands **2c** and **2d** react with CoCl$_2$ to afford Co^{II} zigzag chain coordination polymers **4c** and **4d**, and the CH$_3$CN solvent molecule was trapped within the channel through hydrogen bonds. After activation with MAO, the four nickel complexes show very high catalytic activities for the polymerization of norbornene.

Experimental Section

General Methods and Instrumentation: All manipulations were carried out under an atmosphere of nitrogen by using standard Schlenk and vacuum-line techniques. All solvents were purified and degassed by standard procedures. Norbornene was purchased from ACROS and purified by distillation over sodium. Methylaluminoxane (MAO) was purchased from Aldrich as 10% weight of a toluene solution and used without further purification. Other chemicals were analytical grade and used as received. IR spectra were recorded with a Niclolet AVATAR-360IR spectrometer. Element analyses were performed with an Elementar III vario EI Analyzer. The NMR spectra were obtained by using an ECA-400 spectrophotometer in $CDCl_3$ for compounds with the use of TMS as an internal standard, and *o*-[D$_4$]dichlorobenzene solution for polymers at 120 °C. The intrinsic viscosity [η] was measured in chlorobenzene at 25 °C by using an Ubbelohde viscometer. Viscosity average molecular weight (M_v) values of polymer were calculated by the following equation:[29] $[\eta] = 5.97\times10^{-4}M_v^{0.56}$. The starting materials, 1,1′-dimethyl-3,3-methylenediimidazolium dibromide,[30] 1,1′-(1,2-ethanediyl)bis(3-methyl-imidazolium) dibromide,[30] and $Ni(PPh_3)_2Br_2$[31] were synthesized according to the procedures described in the literature.

Preparation of Ligands and Complexes

Ligand mbit (2a):[4d] $C_9H_{12}N_4S_2$ (240.34): calcd. C 44.98, H 5.03, N 23.31; found C 44.27, H 4.89, N 23.10. ^{1}H NMR (400 MHz, $CDCl_3$): δ = 3.57 (s, 6 H, 2CH$_3$), 6.31 (s, 2 H, CH$_2$), 6.61 (d, 2 H, imidazole), 7.60 (d, 2 H, imidazole) ppm. ^{13}C NMR (100 MHz, $CDCl_3$): δ = 35.21 (CH$_3$), 56.19 (CH$_2$), 117.85 (imidazole), 118.66 (imidazole), 163.71 (C=S) ppm. IR (KBr): $\tilde{\nu}$ = 3162 (m), 3125 (m), 2972 (w), 1656 (w), 1569 (m), 1545 (m), 1461 (s), 1440 (s), 1388 (s), 1372 (s), 1295 (m), 1229 (s), 1161 (m), 1093 (m), 1063 (m), 966 (m), 822 (w), 791 (w), 768 (m), 710 (m) cm^{-1}.

Ligand mbis (2b): In a 100-mL round-bottomed flask fitted with a reflux condenser was placed 1,1-dimethyl-3,3-methylenediimidazolium dibromide (3.38 g, 10 mmol), Se (1.58 g, 20 mmol), K_2CO_3 (1.8 g), and methanol (50 mL) as solvent. The mixture was heated at reflux for 24 h after which the methanol was removed with a rotary evaporator. The remaining solid was taken up in CH_2Cl_2 (2 × 30 mL), and the solution was filtered and the solvent evaporated. Yield: 2.27 g (68%). $C_9H_{12}N_4Se_2$ (334.14): calcd. C 32.35, H 3.62, N 16.77; found C 32.65, H 3.39, N 16.90. ^{1}H NMR (400 MHz, $CDCl_3$): δ = 3.67 (s, 6 H, 2CH$_3$), 6.54 (s, 2 H, CH$_2$), 6.78 (d, 2 H, imidazole), 8.02 (d, 2 H, imidazole) ppm. ^{13}C NMR (100 MHz, $CDCl_3$): δ = 37.33 (CH$_3$), 59.20 (CH$_2$), 119.85 (imidazole), 120.89 (imidazole), 157.87 (C=Se) ppm. IR (KBr): $\tilde{\nu}$ = 3165 (m), 3107 (m), 2983 (m), 2932 (m), 1676 (w), 1566 (m), 1458 (m), 1448 (m), 1386 (s), 1313 (m), 1219 (s), 1194 (m), 1128 (m), 1062 (m), 966 (m), 830 (w), 781 (w), 760 (m), 730 (m) cm^{-1}.

Ligand ebit (2c): The synthesis procedure was similar to that of ligand **2b**.Colorless solid. Yield: 1.9 g (75%). $C_{10}H_{14}N_4S_2$ (254.37): calcd. C 47.22, H 5.55, N 22.03; found C 47.01, H 5.63, N 21.82. ^{1}H NMR (400 MHz, $CDCl_3$): δ = 3.61 (s, 6 H, 2CH$_3$), 4.49 (s, 4 H, CH$_2$-CH$_2$), 6.60 (m, 4 H, imidazole), ^{13}C ppm. NMR (100 MHz, $CDCl_3$): δ = 35.17 (CH$_3$), 45.56 (CH$_2$-CH$_2$), 117.75 (imidazole), 117.83 (imidazole), 162.39 (C=S) ppm. IR (KBr): $\tilde{\nu}$ = 3155 (m), 3119 (m), 3090 (m), 2934 (m), 1632 (w), 1562 (m), 1458 (m), 1443 (m), 1396 (w), 1335 (m), 1242 (m), 1192 (m), 1136 (m), 1083 (m), 830 (m), 744 (m), 703 (m), 674 (m) cm^{-1}.

Ligand ebis (2d): The synthesis procedure was similar to that of ligand **2b**. Colorless solid. Yield: 1.39 g (40%). $C_{10}H_{14}N_4Se_2$ (348.18): calcd. C 34.50, H 4.05, N 16.09; found C 34.78, H 4.27, N 16.24. ^{1}H NMR (400 MHz, $CDCl_3$): δ = 3.69 (s, 2CH$_3$, 6 H), 4.60 (s, CH$_2$, 4 H), 6.78–6.82 (m, imidazole, 4 H), ppm. ^{13}C NMR (100 MHz, $CDCl_3$): δ = 37.17 (CH$_3$), 47.30 (CH$_2$), 119.84 (imidazole), 120.02 (imidazole), 155.80 (C=Se) ppm. IR (KBr): $\tilde{\nu}$ = 3155 (m), 3112 (m), 3082 (m), 2932 (m), 1646 (w), 1560 (m), 1458 (m), 1443 (s), 1402 (w), 1335 (m), 1239 (m), 1171 (m), 1126 (m), 1080 (m), 830 (m), 740 (m), 709 (m), 662 (m) cm^{-1}.

$NiBr_2$mbit (3a): A solution of **2a** (120 mg, 0.5 mmol) and $Ni(PPh_3)_2Br_2$ (372 mg, 0.5 mmol) in CH_2Cl_2 (20 mL) was stirred for 10 h under an atmosphere of nitrogen, resulting in the formation of a dark-green solution and a peak green precipitate. The green product was obtained by filtration and washed with Et_2O (2 × 10 mL) and dried in vacuo for 15 h. Recrystallization of the product from CH_3CN/Et_2O afforded green crystals of **3a** (160 mg, 75%). $C_9H_{12}Br_2N_4NiS_2$ (458.84): calcd. C 23.56, H 2.64, N 12.21; found C 23.58, H 2.49, N 11.96. IR (KBr): $\tilde{\nu}$ = 3157 (m), 3112 (m), 3095 (m), 2970 (w), 1630 (s), 1570 (s), 1470 (m), 1439 (m), 1388 (vs), 1372 (m), 1322 (w), 1235 (m), 1195 (m), 1153 (m), 1092 (m), 1063 (m), 965 (m), 821 (m), 791 (m), 760 (m), 732 (m) cm^{-1}.

$NiBr_2$mbis (3b): The procedure was similar to the synthesis of **3a**. Ligand **2b** and $Ni(PPh_3)_2Br_2$ afforded green crystals of **3b** (110 mg, 40%). $C_9H_{12}Br_2N_4NiSe_2$ (552.64): calcd. C 19.56, H 2.19, N 10.14; found C 20.20, H 2.11, N 10.36. IR (KBr): $\tilde{\nu}$ = 3153 (m), 3107 (m), 2968 (w), 1627 (w), 1570 (s), 1464 (m), 1387 (vs), 1314 (m), 1230 (m), 1194 (m), 1133 (m), 1090 (m), 756 (m), 734 (m), 651 (w) cm^{-1}.

$NiBr_2$ebit (3c): The procedure was similar to the synthesis of **3a**. Ligand **2c** and $Ni(PPh_3)_2Br_2$ afforded green crystals of **3c** (142 mg, 60%). $C_{10}H_{14}Br_2N_4NiS_2$ (472.87): calcd. C 25.40, H 2.98, N 11.85; found C 25.66, H 2.91, N 11.96. IR (KBr): $\tilde{\nu}$ = 3149 (m), 3099 (m), 2975 (w), 1624 (m), 1565 (m), 1480 (s), 1446 (s), 1415 (vs), 1342 (w), 1244 (m), 1193 (m), 1146 (m), 1086 (m), 760 (m), 704 (w), 676 (w) cm^{-1}.

$NiBr_2$ebis (3d): The procedure was similar to the synthesis of **3a**. Ligand **2d** and $Ni(PPh_3)_2Br_2$ afforded kelly-green solid **3d** (90 mg, 32%). $C_{10}H_{14}Br_2N_4NiSe_2$ (566.67): calcd. C 21.20, H 2.49, N 9.89; found C 21.45, H 2.23, N 10.02. IR (KBr): $\tilde{\nu}$ = 3140 (m), 3097 (m), 2939 (m), 1621 (w), 1566 (m), 1475 (s), 1435 (vs), 1402 (m), 1397 (m), 1246 (m), 1171 (w), 1126 (w), 1094 (m), 746 (m), 696 (w), 667 (w) cm^{-1}.

$(CoCl_2\text{mbit})_n$ (4a): A solution of **2a** (125 mg, 0.52 mmol) and $CoCl_2$ (68 mg, 0.52 mmol) in thf (25 mL) was stirred for 24 h under an atmosphere of nitrogen, resulting in the formation of a blue precipitate. The blue solid was obtained by filtration and washed with Et_2O (2 × 20 mL) and dried in vacuo for 24 h. The blue crystal of **4a** was grown from a CH_3CN/Et_2O solution (163 mg, 85%). $C_9H_{12}Cl_2CoN_4S_2$ (370.18): calcd. C 29.20, H 3.27, N 15.13; found C 29.22, H 3.31, N 15.09. IR (KBr): $\tilde{\nu}$ = 3134 (m), 3105 (m), 3012 (m), 2945 (m), 2929 (m), 1568 (m), 1468 (s), 1403 (m), 1328 (m), 1227 (m), 1156 (w), 1075 (m), 1032 (m), 767 (m), 674 (w) cm^{-1}.

$(CoCl_2\text{mbis})_n$ (4b): The procedure was similar to the synthesis of **4a**. Ligand **2b** and $CoCl_2$ afforded blue solid **4b** (135 mg, 56%). The blue crystal of **4b** was grown from a CH_3CN/Et_2O solution. $C_9H_{12}Cl_2CoN_4Se_2$ (463.98): calcd. C 23.30, H 2.61, N 12.08; found C 23.34, H 2.63, N 12.11. IR (KBr): $\tilde{\nu}$ = 3139 (m), 3104 (m), 2964 (m), 2909 (m), 1563 (m), 1386 (s), 1316 (m), 1262 (s), 1227 (m), 1096 (m), 1024 (m), 866 (m), 803 (m), 699 (w) cm^{-1}.

(CoCl$_2$ebit)$_n$ (4c): The procedure was similar to the synthesis of **4a**. Ligand **2c** and CoCl$_2$ afforded blue solid **4c** (137 mg, 69%). The blue crystal of **4c** was grown from a CH$_3$CN/Et$_2$O solution. C$_{10}$H$_{14}$Cl$_2$CoN$_4$S$_2$ (384.21): calcd. C 31.26, H 3.67, N 14.58; found C 31.22, H 3.65, N 14.59. IR (KBr): ṽ = 3142 (m), 3092 (m), 3032 (m), 2945 (m), 1564 (m), 1478 (s), 1409 (m), 1359 (m), 1272 (s), 1249 (m), 1214 (m), 1149 (m), 1097 (m), 962 (m), 758 (m), 683 (w) cm^{-1}.

Table 3. Crystallographic data for Compounds **2c** and **3a–c**.

	2c	**3a**	**3b**	**3c**
Empirical formula	$C_{10}H_{14}N_4S_2$	$C_9H_{12}Br_2N_4NiS_2$	$C_9H_{12}Br_2N_4NiSe_2$	$C_{10}H_{14}Br_2N_4NiS_2$
Formula mass	254.37	458.88	552.68	472.90
Crystal system	Monoclinic	Orthorhombic	Orthorhombic	Monoclinic
Space group	$P2_1/c$	*Pnma*	*Pnma*	$P2_1/n$
a [Å]	4.667(2)	8.203(4)	8.279(3)	10.384(4)
b [Å]	19.705(10)	12.720(6)	12.883(4)	8.510(4)
c [Å]	7.035(3)	14.171(6)	14.465(5)	17.755(7)
α [°]	90	90	90	90
β [°]	107.205(7)	90	90	97.036(6)
γ [°]	90	90	90	90
V [Å^3]	618.0(5)	1478.7(11)	1542.7(9)	1557.2(11)
Z	2	4	4	4
$F(000)$	268	896	1040	928
Crystal size [mm]	0.20 × 0.10 × 0.10	0.15 × 0.10 × 0.10	0.20 × 0.15 × 0.10	0.15 × 0.10 × 0.10
θ range [°]	2.07–26.01	2.15–27.13	2.82–27.11	2.16–27.13
$D_{calcd.}$ [Mg m^{-3}]	1.367	2.061	2.380	2.017
μ [mm^{-1}]	0.410	6.985	11.144	6.637
No. of indep. reflections	2841	6984	7276	7610
No. of obsd. reflections	1214	1697	1776	3418
R_{int}	0.0532	0.0464	0.0328	0.0477
No. of data/restraints/parameters	1214/0/73	1697/0/88	1776/0/89	3418/0/173
Goodness-of-fit on F^2	1.047	1.024	1.019	1.048
R indices (I $>2\sigma$I)^a	R_1 = 0.0594, wR_2 = 0.1494	R_1 = 0.0331 wR_2 = 0.0743	R_1 = 0.0270 wR_2 = 0.0559	R_1 = 0.0518 wR_2 = 0.1212
R indices (all data)	R_1 = 0.0827, wR_2 = 0.1623	R_1 = 0.0450 wR_2 = 0.0789	R_1 = 0.0421 wR_2 = 0.0598	R_1 = 0.0702 wR_2 = 0.1302
$\triangle\rho$(max, min) [e Å^{-3}][a]	0.336, –0.367	0.404, –0.507	0.400, –0.372	1.792, –1.646

[a] $R_1 = \Sigma||F_o| - |F_c||/\Sigma|F_o|$; $wR_2 = [\Sigma w(|F_o{}^2| - |F_c{}^2|)^2/\Sigma w|F_o{}^2|^2]^{1/2}$.

Table 4. Crystallographic data for Compounds **4a–c**.

	4a	**4b**	**4c**
Empirical formula	$C_9H_{12}Cl_2CoN_4S_2$	$C_9H_{12}Cl_2N_4Se_2Co\cdot(H_2O)_{0.67}$	$C_{11}H_{14}Cl_2N_4S_2Co\cdot CH_3CN$
Formula mass	370.18	475.99	425.26
Crystal system	Rhombohedral	Rhombohedral	Monoclinic
Space group	*R*-3*c*	*R*-3*c*	$P2_1/n$
a [Å]	18.902(5)	19.24(3)	7.758(5)
b [Å]	18.902(5)	19.24(3)	16.478(10)
c [Å]	22.178(8)	22.25(4)	15.067(10)
α [°]	90	90	90
β [°]	90	90	104.270(10)
γ [°]	120	120	90
V [Å^3]	6862(4)	7133(20)	1867(2)
Z	18	18	4
$F(000)$	896	4134	868
Crystal size [mm]	0.10 × 0.08 × 0.08	0.12 × 0.10 × 0.08	0.20 × 0.15 × 0.10
θ range [°]	2.22–25.01	2.12–25.01	1.86–27.09
$D_{calcd.}$ [Mg m^{-3}]	1.612	1.995	1.513
μ [mm^{-1}]	1.736	6.006	1.431
No. of indep. reflections	9186	5471	7708
No. of obsd. reflections	1355	1390	4046
R_{int}	0.0877	0.1814	0.0572
No. of data/restraints/parameters	1355/0/84	1390/0/86	4046/0/200
Goodness-of-fit on F^2	1.386	0.858	1.013
R indices (I $>2\sigma$I)^a	R_1 = 0.0870 wR_2 = 0.1458	R_1 = 0.0590 wR_2 = 0.0955	R_1 = 0.0690 wR_2 = 0.1719
R indices (all data)	R_1 = 0.1063 wR_2 = 0.1528	R_1 = 0.1460 wR_2 = 0.1168	R_1 = 0.1098 wR_2 = 0.1910
$\triangle\rho$(max, min) [e Å^{-3}][a]	0.518, –0.489	0.809, –0.690	1.169, –0.410

[a] $R_1 = \Sigma||F_o| - |F_c||/\Sigma|F_o|$; $wR_2 = [\Sigma w(|F_o{}^2| - |F_c{}^2|)^2/\Sigma w|F_o{}^2|^2]^{1/2}$.

$(CoCl_2ebis)_n$ (4d): The procedure was similar to the synthesis of **4a**. Ligand **2d** and $CoCl_2$ afforded blue solid **4d** (134 mg, 54%). $C_{10}H_{14}Cl_2CoN_4Se_2$ (478.01): calcd. C 25.13, H 2.95, N 11.72; found C 25.09, H 2.91, N 11.76. IR (KBr): $\tilde{\nu}$ = 3154 (m), 3115 (m), 2945 (m), 1567 (m), 1475 (m), 1439 (m), 1403 (m), 1368 (s), 1243 (s), 1219 (m), 1186 (m), 1135 (m), 1088 (m), 927 (w), 804 (w), 743 (m), 670 (w) cm^{-1}.

Norbornene Polymerization: In a typical procedure (Table 1, Run 1), nickel complex **3a** (0.2 µmol) in chlorobenzene (2.0 mL), norbornene (3.76 g) in chlorobenzene (6.8 mL), and fresh chlorobenzene (10.0 mL) were added into a special polymerization bottle (50 mL) with a strong stirrer under a nitrogen atmosphere. After the mixture was kept at 25 °C for 10 min, MAO (0.39 mL) was charged into the polymerization system by syringe, and the reaction was started. After 5 min, acidic/ethanol ($V_{ethanol}/V_{concd.HCl}$ = 20:1) was added to terminate the reaction. PNB was isolated by filtration, washed with ethanol, and dried at 80 °C for 36 h under vacuum. For all polymerization procedures, the total reaction volume was 20.0 mL, which can be achieved by the variation of the amount of chlorobenzene when necessary. ^1H NMR (400 MHz, *o*-[D_4]dichlorobenzene): δ = (d 0.7–3.0), (m, maxima at 1.13 1.56 2.11 2.31) ppm. ^{13}C NMR (100 MHz, $CDCl_3$): [maxima at δ (29–33), (34–37), (38–42), (46–53)]. IR (KBr): $\tilde{\nu}$ = 2947 (vs), 2868 (vs), 1474 (m), 1451 (vs), 1373 (m), 1295 (m), 1258 (m), 1222 (m), 1145 (m), 1108 (m), 1040 (w), 943 (w), 893 (m), 804 (m) cm^{-1}.

Crystallographic Structure Determination: Diffraction data for **2c**, **3a–c**, and **4a–c** (Tables 3 and 4) were collected with a Bruker Smart APEX CCD diffractometer with graphite-monochromated Mo-K_{α} radiation (λ = 0.71073 Å). All the data were collected at room temperature and the structures were solved by direct methods and subsequently refined on F^2 by using full-matrix least-squares techniques (SHELXS),[32] SADABS[33] absorption corrections were applied to the data, all non-hydrogen atoms were refined anisotropically, and hydrogen atoms were located at calculated positions. CCDC-660417 (for **2c**), -660418 (for **3a**), -660419 (for **3b**), -660420 (for **3c**), -674279 (for **4a**), -674280 (for **4b**), and -674281 (for **4c**) contain the supplementary crystallographic data for this paper. These data can be obtained free of charge from The Cambridge Crystallographic Data Centre via www.ccdc.cam.ac.uk/data_request/cif.

Acknowledgments

Financial support by the National Science Foundation of China (20531020, 20721063, 20771028), Shanghai Leading Academic Discipline project (B108), National Basic Research Program of China (2005CB623800), and Shanghai Science and Technology Committee (06XD14002) is gratefully acknowledged.

---

[1] a) R. G. Pearson, *J. Am. Chem. Soc.* **1963**, *85*, 3533–3539; b) R. M. Silva, M. D. Smith, J. R. Gardinier, *Inorg. Chem.* **2006**, *45*, 2132–2142; c) R. G. Pearson (Ed.), *Hard and Soft Acids and Bases*, Dowden, Hutchinson & Ross, Stroudsburg, PA, **1973**.

[2] See for example: a) L. Han, B. Wu, Y. Xu, Y. Gong, B. Lou, B. Chen, M. Hong, *Inorg. Chim. Acta* **2005**, *358*, 2005–2013; b) Y. B. Xie, C. Zhang, J. R. Li, X. H. Bu, *Dalton Trans.* **2004**, 562–569; c) S. Liu, Y. F. Han, G.-X. Jin, *Chem. Soc. Rev.* **2007**, *36*, 1543–1560.

[3] a) G. Parkin, *Chem. Rev.* **2004**, *104*, 699–768; b) H. Vahrenkamp, *Acc. Chem. Res.* **1999**, *32*, 589–596; c) M. O. Awaleh, A. Badia, F. Brisse, *Inorg. Chem.* **2005**, *44*, 7833–7845.

[4] a) F. Bigoli, P. Deplano, F. A. Devillanova, V. Lippolis, M. L. Mercuri, M. A. Pellinghelli, E. F. Trogu, *Inorg. Chim. Acta* **1998**, *267*, 115–121; b) F. P. Bigoli, P. Deplano, M. L. Mercuri, M. A. Pellinghelli, A. Sabatini, E. F. Trogu, A. Vacca, *J. Chem. Soc., Dalton Trans.* **1996**, 3583–3590; c) D. J. Williams, A. Shilatifard, D. VanDerveer, L. A. Lipscomb, R. L. Jones, *Inorg. Chim. Acta* **1992**, *202*, 53–57; d) D. J. Williams, D. VanDerveer, R. L. Jones, D. S. Menaldino, *Inorg. Chim. Acta* **1989**, *165*, 173–178; e) L. S. Bark, N. Chadwick, O. Meth-Cohn, *Tetrahedron* **1992**, *48*, 7863–7868; f) R. M. Silva, M. D. Smith, J. R. Gardinier, *J. Org. Chem.* **2005**, *70*, 8755–8763; g) I. R. Crossley, A. F. Hill, E. R. Humphrey, M. K. Smith, *Organometallics* **2006**, *25*, 2242–2247; h) L. Maria, C. Moura, A. Paulo, I. C. Santos, I. Santos, *J. Organomet. Chem.* **2006**, *691*, 4773–4778.

[5] a) R. Kato, *Chem. Rev.* **2004**, *104*, 5319–5346; b) X. Wang, G.-X. Jin, *Organometallics* **2004**, *23*, 6319–6322; c) D. J. Hamison, N. Nguyen, A. J. Lough, U. Fekl, *J. Am. Chem. Soc.* **2006**, *128*, 11026–11027; d) W. E. Geiger, *Inorg. Chem.* **2002**, *41*, 136–139; e) Y. K. Han, D. K. Seo, H. Y. Kang, W. Kang, D. Y. Noh, *Inorg. Chem.* **2004**, *43*, 7294–7300; f) B. S. Lim, D. V. Fomitchev, R. H. Holm, *Inorg. Chem.* **2001**, *40*, 4257–4262; g) T. Waters, H. K. Woo, X. B. Wang, L. S. Wang, *J. Am. Chem. Soc.* **2006**, *128*, 4282–4291; h) S. X. Liu, C. Ambrus, S. Dolder, A. Neels, S. Decurtins, *Inorg. Chem.* **2006**, *45*, 9622–9624; i) Y. Kosaka, H. M. Yamamoto, A. Nakao, M. Tamura, R. Kato, *J. Am. Chem. Soc.* **2007**, *129*, 3054–3055; j) H. Kisch, B. Eisen, R. Dinnebier, K. Shankland, W. I. F. David, F. Knoch, *Chem. Eur. J.* **2001**, *7*, 738–748.

[6] a) M. Minoura, V. K. Landry, J. G. Melnick, K. L. Pang, L. Marchio, G. Parkin, *Chem. Commun.* **2006**, *38*, 3990–3992; b) V. K. Landry, D. Buccella, K. L. Pang, G. Parkin, *Dalton Trans.* **2007**, 866–870; c) V. K. Landry, G. Parkin, *Polyhedron* **2007**, *26*, 4751–4757.

[7] I. Tritto, L. Boggioni, M. C. Sacchi, P. Locatelli, *J. Mol. Catal. A* **1998**, *133*, 139–150.

[8] W. Kaminsky, A. Bark, M. Arndt, *Makromol. Chem. Macromol. Symp.* **1991**, *47*, 83–93.

[9] M. J. Brekner, H. Decker, F. Osan (Hoechst AG), EP Patent **1994**, *683*, 797.

[10] R. J. Minchak, J. T. Ware (B. F. Goodrich), EP Patent **1988**, *291*, 970.

[11] a) J. X. Chen, Y. B. Huang, Z. S. Li, Z. C. Zhang, C. X. Wei, T. Y. Lan, W. J. Zhang, *J. Mol. Catal. A* **2006**, *259*, 133–141; b) B. L. Goodall, L. H. McIntosh III, L. F. Rhodes, *Makromol. Chem. Macromol. Symp.* **1995**, *89*, 421–432; c) H. Yasuda, Y. Nakayama, Y. Sato, *J. Organomet. Chem.* **2004**, *689*, 744–750; d) P. Frédéric, J. L. Pierre, W. Marcel, K. Jacky, *Macromol. Rapid Commun.* **2003**, *24*, 768–771.

[12] a) U. Peuckert, W. Heitz, *Macromol. Rapid Commun.* **1998**, *19*, 159–162; b) P. G. Lassahn, V. Lozan, G. A. Timco, P. Christian, C. Janiak, E. P. Winpenny, *J. Catal.* **2004**, *222*, 260–267.

[13] a) H. Y. Wang, G.-X. Jin, *Eur. J. Inorg. Chem.* **2005**, *9*, 1665–1670; b) L. Bourget-Merle, M. Lappert, J. R. Severn, *Chem. Rev.* **2002**, *102*, 3031–3066; c) H. Y. Wang, X. Meng, G.-X. Jin, *Dalton Trans.* **2006**, 2579–2585; d) H. Gao, W. Guo, F. Bao, G. Gui, J. Zhang, F. Zhu, Q. Wu, *Organometallics* **2004**, *23*, 6273–6280; e) D. A. Barnes, G. M. Benedikt, B. L. Goodall, S. S. Huang, H. A. Kalamarides, S. Lenhard, L. H. McIntosh III, K. T. Selvy, R. A. Shick, L. F. Rhodes, *Macromolecules* **2003**, *36*, 2623–2632; f) V. Lozan, P. G. Lassahn, C. Zhang, B. Wu, C. Janiak, G. Rheinwald, H. Z. Lang, *Z. Naturforsch. B: Chem. Sci.* **2003**, *58*, 1152–1164; g) C. Janiak, P. G. Lassahn, *J. Mol. Catal. A* **2001**, *166*, 193–209; h) Y. Z. Zhu, J. Y. Liu, Y. S. Li, Y. J. Tong, *J. Organomet. Chem.* **2004**, *689*, 1295–1303; i) J. X. Hou, W. H. Sun, D. H. Zhang, L. Y. Chen, *J. Mol. Catal. A* **2005**, *231*, 221–233; j) F. Chang, D. Zhang, G. Y. Xu, H. J. Yang, J. T. Li, H. B. Song, W. H. Sun, *J. Organomet. Chem.* **2004**, *689*, 936–946; k) H. Suzuki, S. Matsumura, Y. Satoh, K. Sogoh, H. Yasuda, *React. Funct. Polym.* **2004**, *58*, 77–91; l) X. Mi, Z. Ma, N. Cui, L. Wang, Y. Ke, Y. Hu, *J. Appl. Polym. Sci.* **2003**, *88*, 3273–3278; m) X. Wang, S. Liu, G.-X. Jin, *Organometallics* **2004**, *23*, 6002–6007; n) W. H. Wang, G.-X. Jin,

Inorg. Chem. Commun. **2005**, *8*, 109–112; o) Y. B. Huang, G. R. Tang, G. Y. Jin, G.-X. Jin, *Organometallics* **2008**, *27*, 259–269; p) F. T. Chen, G. R. Tang, G.-X. Jin, *J. Organomet. Chem.* **2007**, *692*, 3435–3442.

[14] a) C. Mehler, W. Risse, *Macromolecules* **1992**, *25*, 4226–4228; b) P. G. Lassahn, V. Lozan, C. Janiak, *Dalton Trans.* **2003**, 927–935; c) B. Berchtold, V. Lozan, P. G. Lassahn, C. Aniak, *J. Polym. Sci. A: Polym. Chem.* **2002**, *40*, 3604–3614.

[15] a) C. Carlini, S. Giaiacopi, F. Marchetti, C. Pinzino, A. M. R. Galletti, G. Sbrana, *Organometallics* **2006**, *25*, 3659–3664; b) A. M. R. Galletti, C. Carlini, S. Giaiacopi, M. Marco, S. Glauco, *J. Polym. Sci. Part A: Polym. Chem.* **2007**, *45*, 1134–1142; c) X. Q. Lü, F. Bao, B. S. Kang, Q. Wu, H. Q. Liu, F. M. Zhu, *J. Organomet. Chem.* **2006**, *691*, 821–828; d) G. R. Tang, Y. J. Lin, G.-X. Jin, *J. Organomet. Chem.* **2007**, *692*, 4106–4112; e) M. Karl, G. Seybert, W. Massa, K. Harms, S. Agarwal, R. Maleika, W. Stelter, A. Greiner, W. Heitz, B. Neumuller, K. Z. Dehnicke, *Z. Anorg. Allg. Chem.* **1999**, *625*, 1301–1309.

[16] T. J. Deming, B. M. Novak, *Macromolecules* **1993**, *26*, 7089–7091.

[17] a) G. J. P. Britovsek, V. C. Gibson, D. F. Wass, *Angew. Chem. Int. Ed.* **1999**, *38*, 428–447; b) S. D. Ittel, L. K. Johnson, M. Brookhart, *Chem. Rev.* **2000**, *100*, 1169–1204; c) V. C. Gibson, S. K. Spitzmesser, *Chem. Rev.* **2003**, *103*, 283–316; d) L. S. Boffa, B. M. Novak, *Chem. Rev.* **2000**, *100*, 1479–1494; e) F. Speiser, P. Braunstein, L. Saussine, *Acc. Chem. Res.* **2005**, *38*, 784–793; f) J. Zhang, X. Wang, G.-X. Jin, *Coord. Chem. Rev.* **2006**, *250*, 95–109.

[18] a) H. S. Schrekker, V. Kotov, P. Preishuber-Pflugl, P. White, M. Brookhart, *Macromolecules* **2006**, *39*, 6341–6354; b) A. Buchard, A. Auffrant, C. Klemps, L. Vu-Do, L. Boubekeur, X. F. Le Goff, P. L. Floch, *Chem. Commun.* **2007**, 1502–1504; c) L. Boubekeur, L. Ricard, N. Mézailles, P. L. Floch, *Organometallics* **2005**, *24*, 1065–1074; d) J. M. Benito, E. de Jesús, F. Javier de la Mata, J. C. Flores, R. Gómez, *Chem. Commun.* **2005**, 5217–5219; e) X. B. Tang, D. H. Zhang, S. Y. Jie, W. H. Sun, J. T. Chen, *J. Organomet. Chem.* **2005**, *690*, 3918–3928; f) X. B. Tang, W. H. Sun, T. L. Gao, J. X. Hou, J. T. Chen, W. Chen, *J. Organomet. Chem.* **2005**, *690*, 1570–1580; g) K. Nienkemper, V. V. Kotov, G. Kehr, G. Erker, R. Fröhlich, *Eur. J. Inorg. Chem.* **2006**, *2*, 366–379; h) M. E. Bluhm, C. Folli, O. Walter, M. Dŏring, *J. Mol. Catal. A* **2005**, *229*, 177–181.

[19] V. K. Landry, M. Minoura, K. L. Pang, D. Buccella, B. V. Kelly, G. Parkin, *J. Am. Chem. Soc.* **2006**, *128*, 12490–12497.

[20] M. Nomura, M. Geoffroy, P. Adkine, M. Fourmigue, *Eur. J. Inorg. Chem.* **2006**, *24*, 5012–5021.

[21] M. Nomura, T. Cauchy, M. Geoffroy, P. Adkine, M. Fourmigue, *Inorg. Chem.* **2006**, *45*, 8194–8204.

[22] S. Senda, Y. Ohki, T. Hirayama, D. Toda, J. L. Chen, T. Matsumoto, H. Kawaguchi, K. Tatsumi, *Inorg. Chem.* **2006**, *45*, 9914–9925.

[23] M. Fourmigue, N. Avarvari, *Dalton Trans.* **2005**, *8*, 1365–1371.

[24] V. K. Landry, K. L. Pang, S. M. Quan, G. Parkin, *Dalton Trans.* **2007**, *8*, 820–824.

[25] R. H. Wang, L. Han, L. J. Xu, Y. Q. Gong, Y. F. Zhou, M. C. Hong, A. S. C. Chan, *Eur. J. Inorg. Chem.* **2004**, 3751–3763.

[26] J. P. Kennedy, H. S. Makowski, *J. Macromol. Sci. (Chem.) A1* **1967**, 345–370.

[27] a) M. Arndt, R. Engehausen, W. Kaminsky, K. Zoumis, *J. Mol. Catal. A* **1995**, *101*, 171–178; b) T. Tsujino, T. Saegusa, J. Furukawa, *Die Mkromol. Chem.* **1965**, *85*, 71–79.

[28] C. Mast, M. Krieger, K. Dehnicke, A. Greiner, *Macromol. Rapid Commun.* **1999**, *20*, 232–235.

[29] T. F. A. Haselwander, W. Heitz, M. Maskos, *Macromol. Rapid Commun.* **1997**, *18*, 689–697.

[30] W. A. Herrmann, J. Schwarz, *Organometallics* **1999**, *18*, 4082–4089.

[31] Z. Trávnícek, V. Machala, L. Szücvá, M. Maloň, J. Marek, *Transition. Met. Chem.* **2004**, *29*, 352–357.

[32] G. M. Sheldrick, *SHELXL-97: Program for the Refinement of Crystal Structures*, University of Göttingen, Germany, **1997**.

[33] G. M. Sheldrick, *SADABS* (*2.01*), *Bruker/Siemens Area Detector Absorption Correction Program*, Bruker AXS, Madison, Wisconsin, USA, **1998**.

Received: June 2, 2008